

Electronic states and transport in quasicrystals investigated by perturbation theory

Jochen Peters and Hans-Rainer Trebin

Institut für Theoretische und Angewandte Physik, Universität Stuttgart, Pfaffenwaldring 57, D-70550 Stuttgart, Germany

(Received 14 September 1994)

The electronic properties of quasicrystals are exotic due to the unusual combination of long-range structural order and nonperiodicity. This article complements previous work about the electronic states of linear quasicrystals and their successive rational approximants using perturbation theory instead of the common transfer-matrix method. The wave functions of large approximants can frequently be decomposed into building blocks which essentially represent corresponding states of lower approximants. This behavior is discussed using a simple approximate description of the envelopes of the wave functions. To describe electronic transport properties we present a perturbation theory for the Landauer resistance. The Lyapunov exponents describing its growth with sample length are interpreted in terms of the samples' Fourier spectra. We conclude with a discussion of the increasingly complex energy dependence of the resistance as we grow larger samples.

I. INTRODUCTION

Since the experimental discovery of quasicrystals in the mid 1980s,¹⁻³ their structure and their electronic properties have attracted much interest. Bearing in mind the metallic ingredients of quasicrystalline alloys, the following experimental results are remarkable.⁴⁻¹¹ Room temperature resistivities exceed typical values for pure metals by at least three orders of magnitude. They are particularly high for thermodynamically stable quasicrystals. Reducing thermal or intrinsic disorder by cooling or annealing the specimens *increases* the resistivity. Strong magnetoresistances of both positive and negative sign are observed. Frequently nonlinear temperature dependences of the thermopower and strong variations of the Hall coefficient with temperature complete the puzzle. Some of the data can be modeled using the concepts of weak localization and electron-electron interaction, originally devised for *disordered* systems. Regarding the long-range order of quasicrystals, however, the use of these concepts is barely motivated here. Furthermore, a consistent picture accounting for *all* the observed anomalies is still missing.^{4,7,10,12}

The correlation between resistance and structural order (and stability) suggests a fundamental, possibly new connection between the unusual quasiperiodic structure and the electronic properties. Actually, research concerning basic properties of quasiperiodic Hamiltonians already boomed before the discovery of quasicrystals¹³⁻¹⁶ and was further stimulated by the experimental findings. While some numerical work was done on two- and three-dimensional Penrose clusters, all analytical approaches hitherto are restricted to linear systems. Most analytical results describe the singular continuous energy spectra, whereas only few statements are given about the energy dependence of the Landauer resistance and about the structure of the wave functions.^{5,13-30} The latter are always calculated for "rational approximants" and we shall follow this approach. Comparing related states for *successive approximants*, we find a hierarchical structure of

the generic type of wave functions which is not evident in a single approximant. This complements previous work on selected, self-similar states and on multifractal analyses of the generic, seemingly "chaotic" wave functions.

The outline is as follows. In Sec. II a Green-function-like reformulation of perturbation theory for periodic Schrödinger operators will be presented as a tool box for the following investigations. This will allow us to calculate wave functions and Landauer resistances without resort to the usual transfer-matrix method.¹⁶⁻³⁰ In Sec. III we shall apply the new formalism to a Kronig-Penney model for rational approximants. Using a new, approximate expression for the envelopes of the wave functions, we shall discuss the above mentioned structural hierarchy. Section IV is devoted to an analysis of the Landauer resistance R_L . Looking at the growth of R_L with sample length we derive a rule of thumb which establishes a simple one-to-one correspondence between the Lyapunov exponents of R_L and the approximants' Fourier spectra. Finally the extreme R_L fluctuations with varying energy will be discussed. These investigations complement perturbation theoretical analyses by Luck and Barache^{31,32} of the electronic spectra and the integrated density of states of deterministic aperiodic systems.

II. PERTURBATION THEORY IN REAL SPACE

Let us consider the one-particle Schrödinger equation

$$\left[-\frac{d^2}{dx^2} + V(x) \right] \psi(x) = E \psi(x), \quad (1)$$

with $[-\frac{d^2}{dx^2}]$ as the unperturbed Hamiltonian and $V(x)$ as perturbation. The potential is assumed to be P periodic, so that it takes the form

$$V(x) = \sum_{m \in \mathbb{Z}} \hat{V}_m \exp(i \frac{2\pi m}{P} x).$$

For spectral energies we can concentrate on Bloch functions with the property

$$\psi(x + P) = \psi(x) \exp(i k_0 P).$$

For gap energies the solutions grow exponentially as $x \rightarrow \infty$ or $x \rightarrow -\infty$. Usually, these non-normalizable solutions are ignored, but we shall need them for estimating the electronic transmission properties of *finite* samples in Sec. IV. From transfer-matrix considerations one can immediately conclude that for each energy of the ℓ th gap there exists a pair ψ_{\pm} of solutions with the property

$$\begin{aligned} \psi_{\pm}(x + P) &= \psi_{\pm}(x) \exp[(i k_0 \pm \kappa) P], \\ k_0 &= \frac{\ell\pi}{P}, \quad \kappa \in \mathbb{R}. \end{aligned} \quad (2)$$

As we approach the gap edges, κ goes to zero.

A. Nondegenerate case (inside the bands)

As usual, ψ and E are expanded into series

$$\begin{aligned} \psi &= \psi^{(0)} + \psi^{(1)} + \psi^{(2)} + \dots, \\ E &= E^{(0)} + E^{(1)} + E^{(2)} + \dots, \end{aligned} \quad (3)$$

where $\psi^{(n)}$ and $E^{(n)}$ are of the order $O(V^n)$. The unperturbed problem is solved by

$$\psi^{(0)}(x) = \exp(i k_0 x), \quad E^{(0)} = k_0^2. \quad (4)$$

For the sake of clarity we postpone the basic calculations to the Appendix and simply quote the first- and second-order corrections

$$\psi^{(1)}(x) = \int_0^P b(x') [V\psi^{(0)}](x - x') dx', \quad (5)$$

$$E^{(1)} = \frac{1}{P} \int_0^P V(x) dx = \hat{V}_0, \quad (6)$$

$$\psi^{(2)}(x) = \int_0^P b(x') [(V - E^{(1)})\psi^{(1)}](x - x') dx', \quad (7)$$

$$E^{(2)} = \frac{1}{P} \int_0^P V(x) \psi^{(1)}(x) \exp(-i k_0 x) dx, \quad (8)$$

with the “band kernel”

$$b(x) = \exp(i k_0 x) \left\{ \frac{-1}{4Pk_0^2} + i \frac{2x - P}{4Pk_0} + \frac{\exp[i k_0 (P - 2x)]}{4k_0 \sin(Pk_0)} \right\}. \quad (9)$$

This formalism is similar to the Born series in scattering theory for spatially bounded potentials. Note that instead of using a Green function for fixed energy, the Bloch wave vector is held fixed here. This gives rise to the energy correction term in $\psi^{(2)}$. Furthermore, rather than integrating over the whole support of $V(x)$, the integrals (5) and (7) are restricted to one period (thus guaranteeing convergence).

B. Degenerate case (band edges and gaps)

For the sake of compactness we shall interpret the band edges as *gap edges* by simply requiring $\kappa = 0$ in (2). To adequately describe the diverging states within the gaps, we make the following ansatz:

$$\psi(x) =: \exp(\kappa x) w(x), \quad (10)$$

$$w(x + P) = w(x) \exp(i k_0 P), \quad k_0 = \frac{\ell\pi}{P}. \quad (11)$$

Now perturbation series are derived for w and κ (instead of ψ) and for E . To keep the results simple, we shall assume that $V(x)$ has a center of symmetry x_s , which is the case for any approximant of a quasilattice projected from two dimensions to one dimension. Then the Fourier coefficients of the potential with respect to x_s are real:

$$\hat{V}_\ell^s := \hat{V}_\ell \exp(i \frac{2\pi\ell}{P} x_s) = \pm |\hat{V}_\ell|. \quad (12)$$

The suitable zero order solutions are of the form

$$\begin{aligned} w^{(0)}(x) &= \text{trig} \left[k_0 (x - x_s) - \frac{\phi}{2} \right], \\ \kappa^{(0)} &= 0, \quad E^{(0)} = k_0^2, \end{aligned} \quad (13)$$

with $\text{trig} := \cos$ (\sin) for $\hat{V}_\ell^s > 0$ (< 0). The parameter $\phi \in (-\pi, \pi]$ labels the different states within the ℓ th gap. The special values $\phi = 0, \pi$ correspond to the gap edges where κ will vanish identically in any order. The first order reads

$$w^{(1)}(x) = \int_0^P g(x') [Vw^{(0)}](x - x') dx', \quad (14)$$

$$\kappa^{(1)} = \frac{|\hat{V}_\ell|}{2k_0} \sin \phi, \quad (15)$$

$$E^{(1)} = \hat{V}_0 + |\hat{V}_\ell| \cos \phi, \quad (16)$$

with the “gap kernel”

$$g(x) = \frac{-\cos(k_0 x)}{2Pk_0^2} + \sin(k_0 x) \frac{P - 2x}{2Pk_0}. \quad (17)$$

The second order is slightly more complicated than (7) and (8) due to terms with $\kappa^{(1)}$. For the general n th order expressions we refer to the Appendix.

Note that in (15) and (16) a pair of parameters $\{\phi, -\phi\}$ corresponds to a single energy and a pair $\{\kappa, -\kappa\}$ in agreement with (2). Moreover, plotting κ versus E results in ellipses of height $|\hat{V}_\ell|/k_0$ and width $2|\hat{V}_\ell|$. Such elliptic structures for the “inverse localization length” have been reported (but not explained) by Würtz *et al.*²³ We shall return to this observation in Sec. IV.

III. STRUCTURE OF THE WAVE FUNCTIONS

As a particularly simple model we shall discuss the Kronig-Penney potential

$$V(x) = V \sum \delta(x - x_n),$$

where x_n runs through the vertices of the considered quasicrystal or its approximants. Besides from reducing the integrals of Sec. II to *sums*, this model is easily treated numerically via transfer matrices (TM's). This facilitates the comparison of perturbative versus exact results.

In the following we concentrate on $p:q$ approximants, i.e., on periodic structures with p (q) interatomic distances ($x_{n+1} - x_n$) of length L (S) in the elementary cell. We recall the concatenation rule for the construction of successive approximants. Let $p_m:q_m$ ($m=0,1,2,\dots$) be a series of continued fractions converging towards the $L:S$ stoichiometry of the considered quasicrystal:

$$\frac{p_m}{q_m} = a_0 + \frac{1}{a_1 + \frac{1}{a_2 + \dots + \frac{1}{a_m}}} \quad (a_i \in \mathbb{N}) \quad (18)$$

and let C_m be a suitably chosen elementary cell of the m th approximant. Then the following holds:^{33,34}

$$C_0 = L^{a_0} \circ S, \quad C_1 = C_0^{a_1} \circ L, \quad C_m = C_{m-1}^{a_m} \circ C_{m-2}, \quad (19)$$

where C^a denotes the a -fold repetition of C and \circ signifies the concatenation. The special case $a_i = 1 \forall i$ yields the well-known *Fibonacci approximants*.

As mentioned in the Introduction, most of the Bloch states of higher approximants lack a lucid structure. The comparison of *successive approximants*, however, frequently shows a "structural heredity" of the states with similar k_0 . This point is illustrated in Fig. 1: Partial structures of the 21:13 wave function reappear in the 34:21 and the 55:34 states, while a large 34:21 fragment shows up in the 55:34 state. Quite generally the similarity of corresponding states is maximal in the vicinity of the symmetry centers of the approximants. The three possible types of these symmetry points are indicated in Fig. 1: A type A center bisects an S interval, type B bisects an L , and C lies between two adjoining L 's.³⁵ It can be shown that any pair of approximants has one center of common type. Moreover, due to the concatenation rule (19), the L - S sequences in the vicinity of the common centers are identical over at least one period of the shorter approximant (e.g., $\geq \frac{34}{2}$ to both sides of B if you compare the 21:13 and the 55:34 approximant). This fact turns out to cause the frequently observed transfer of local ψ patterns from one approximant to higher ones.

In order to get a simple model of this behavior we now eliminate the rapid ψ oscillations and restrict the discussion to the envelopes of the wave functions. Let us recall the ansatz always used in TM calculations:

$$\psi(x) = A(x) \exp(i\sqrt{E}x) + B(x) \exp(-i\sqrt{E}x), \quad (20)$$

with $A(x) = \text{const}$ and $B(x) = \text{const}$ between the peaks of the potential. Obviously, $|\psi|$ oscillates between

$$||A| - |B|| \leq |\psi| \leq |A| + |B|.$$

These lower and upper envelopes are readily calculated using TM's. The steplike curves are much easier to grasp

and to compare visually than $|\psi|$ itself, but the TM algorithm hampers the discussion of their shape. This is why we employ perturbation theory to get a more "transparent" approximate expression, which facilitates the discussion of the ψ shapes.

A crucial observation is that from the knowledge of $\psi(x)$ and E we can deduce $A(x)$ and $B(x)$:

$$A(x) \exp(i\sqrt{E}x) = \frac{1}{2} \psi(x) + \frac{1}{2i\sqrt{E}} \frac{d\psi}{dx}. \quad (21)$$

Similarly, $B(x) \exp(-i\sqrt{E}x)$ results from subtracting

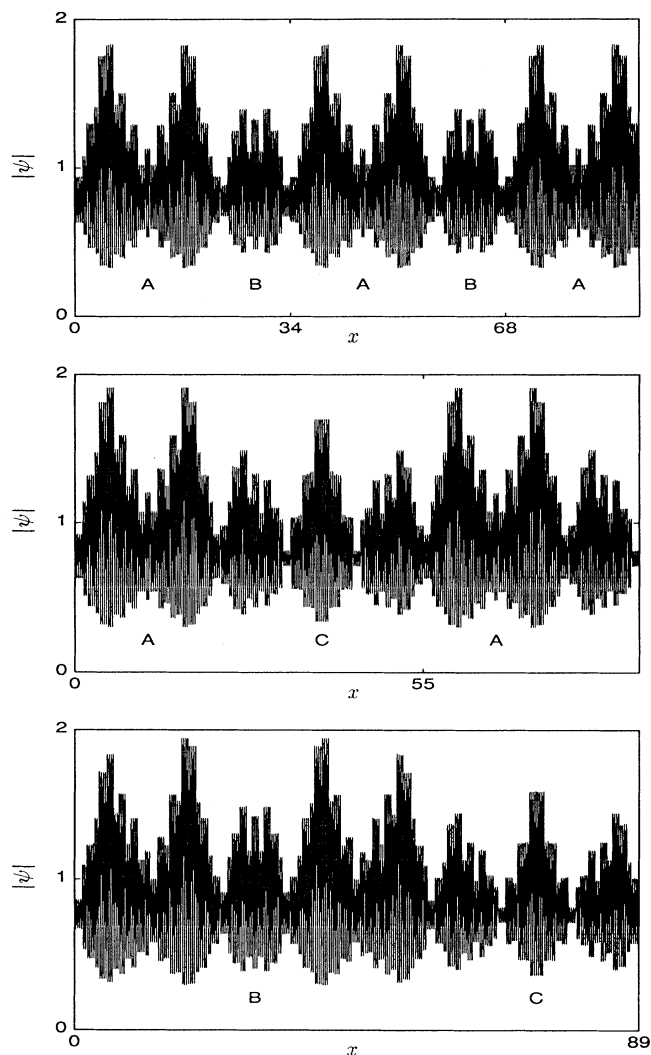


FIG. 1. Normalized states for the Fibonacci approximants 21:13, 34:21, and 55:34 from the 107th, the 173rd, and the 280th band, respectively. The respective periods are indicated on the x axis. The letters A, B, and C label the different centers of symmetry; see the text. The structure of the 21:13 wave function within the interval ABA can be identified with the corresponding B surroundings in the 55:34 approximant. Similarly, the ACA part from 34:21 reappears around C in 55:34. The A-centered ψ structure is common to the 21:13 and the 34:21 approximant. (For comparison Fig. 2 shows the second-order approximation of the 55:34 wave function.)

the second term. Now, since we know the series for ψ and E we can derive perturbation series for A and B . Here we restrict our discussion to *band states* (excluding the band edges). From (5) and (6) we get the following expressions for their *absolute values* (without normalization):³⁴

$$|A(x)| \stackrel{\text{first}}{=} 1 - \frac{\hat{V}_0}{4k_0^2} = \text{const}, \quad (22)$$

$$|B(x)| \stackrel{\text{first}}{=} \frac{|\int_x^{x+P} V(x') \exp(2i k_0 x') dx'|}{|4k_0 \sin(Pk_0)|}. \quad (23)$$

Note that $|B|$ depends on x via the integral's limits. The second-order expressions look much more complicated, but the basic message is the following: (i) The shape of $|A|$ is brought into line with the form of $|B|$ given in (23). The absolute fluctuations of $|A|$, however, are smaller than those of $|B|$.³⁶ (ii) Generally, the overall form of $|B(x)|$ does not change very much, although the second order may introduce some minor local adjustments. Summarizing, the first-order expression (23) governs the structure of both $|A|$ and $|B|$. This behavior is illustrated in Fig. 3 for the 55:34 state of Fig. 1.

So we end up with the following rule of thumb to estimate the shape of a band state of a P -periodic approximant. First, the "truncated Fourier transform" of the potential

$$\mathcal{F}(x, k_0) := \left| \int_x^{x+P} V(x') \exp(2i k_0 x') dx' \right|$$

gives $|B(x)|$ to first order, except for a constant factor. Second, since the shape of $|A|$ resembles that of $|B|$, the *upper envelope* $|A|+|B|$ is *essentially characterized* by \mathcal{F} .

This function is much easier to discuss than the TM recipe for ψ , A , and B . It can be shown that the concatenation rule (19) results in a correlation of the functions $\mathcal{F}(x)$ for successive approximants. Furthermore, the similarity of corresponding \mathcal{F} curves is maximal in

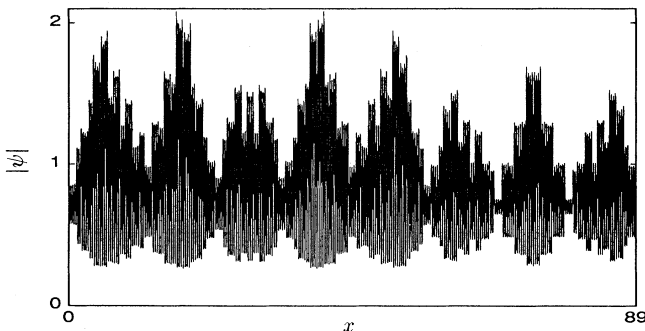


FIG. 2. The last state of Fig. 1 is approximated to second order using (5)–(7) (and normalized) using the same parameters $k_0 = \frac{279.5\pi}{89}$ and $V = 5$ as in Fig. 1. Although $|\psi|$ appears to be a little more fuzzy than the exact state, the general agreement is quite satisfactory. [The first order does not yield an acceptable approximation. This is due to the lack of any spatial structure of the coefficient $|A|$ in Eq. (22); see also the first plot of Fig. 3.]

the vicinity of the common symmetry centers discussed in Fig. 1.³⁴ We have thus made plausible the observed ψ transfer from one approximant to the higher ones.

As a consequence, as we proceed to larger and larger approximants we arrive at increasingly complex patterns, each containing fragments of the wave functions of the next lower approximants, which in turn are composed of building blocks from even lower approximants and so on. This scenario is illustrated in Fig. 4.

We point out that our conclusions apply to *any* sequence of approximants described by (18) and (19) and are not restricted to the slowly growing Fibonacci series used in the illustrations. Similar results can also be derived for the band edge states, but the involved formulas are slightly more complicated, so that we refrain from a deeper discussion here.

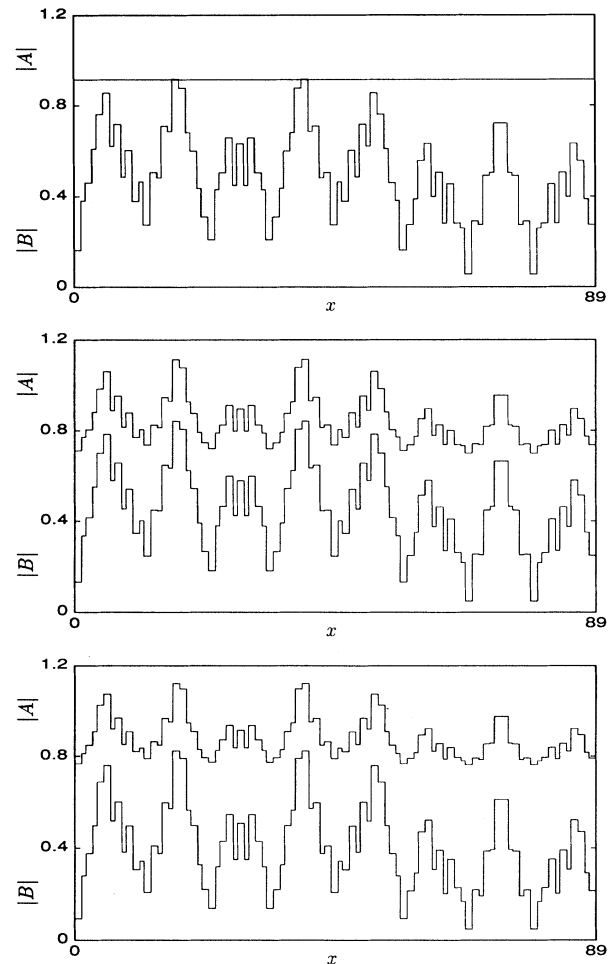


FIG. 3. The curves $|A(x)|$ and $|B(x)|$ are plotted for the last state of Fig. 1; see also Fig. 2. The upper and lower envelopes of $|\psi|$ are given as the sum and the difference of $|A|$ and $|B|$. The top and middle plots illustrate the first and the second order of perturbation theory, respectively. The bottom plots were calculated using the TM method. Note that the first order for $|B|$ almost perfectly matches the correct shape, while the second order is needed to approximate the exact $|A|$ curve.

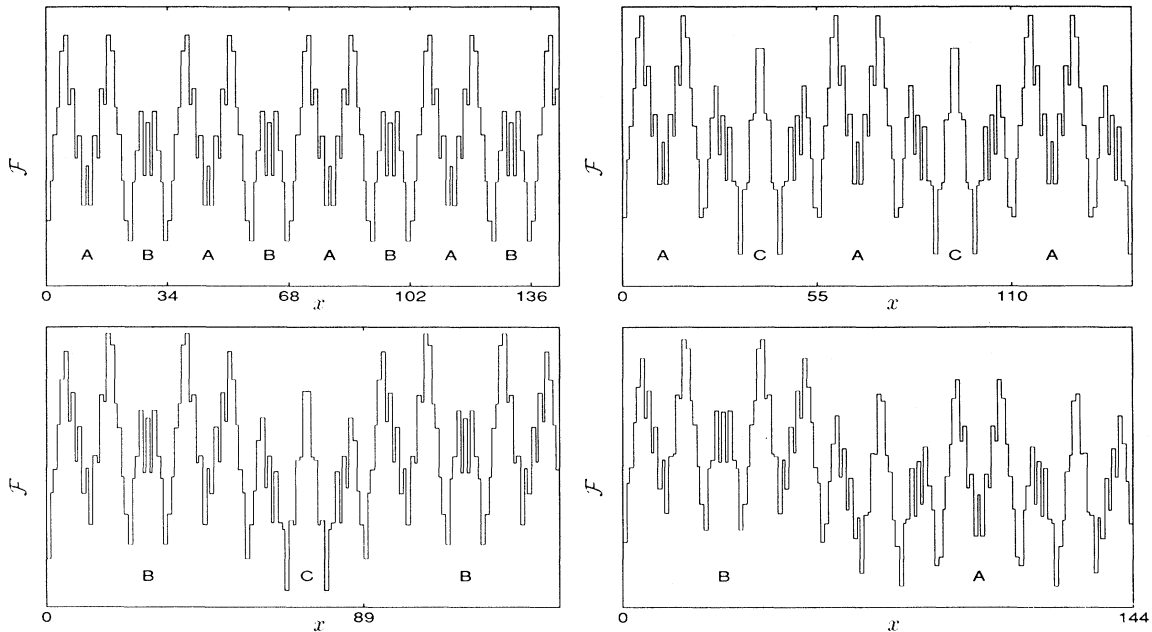


FIG. 4. Comparison of the \mathcal{F} curves for the approximants of Fig. 1, supplemented by the 89:55 approximant. As in Fig. 1, the wave vectors k_0 equal $\frac{106.8\pi}{34}$, $\frac{172.7\pi}{55}$, $\frac{279.5\pi}{89}$, and (new) $\frac{452.5\pi}{144}$. The structural heredity of the growing A, the B, and the C surroundings from lower to higher approximants is clearly visible. [The scaling of the first three plots includes a factor $|\sin(Pk_0)|^{-1}$; cf. Eq. (23). The ordinate of the last plot is slightly compressed.]

IV. LANDAUER RESISTANCE

To characterize the electronic transport of linear samples in the absence of thermal disorder it has become customary to investigate the scattering of monochromatic electrons by the sample. The ratio of reflection to transmission defines the Landauer resistance R_L (up to a constant factor). Sutherland and Kohmoto²⁰ pointed out that the interpretation as a resistance is questionable in the case of quasicrystals (due to the Cantor-set spectra with gaps all over). Nevertheless, R_L as a function of the energy of the incident electrons shows interesting features. Characteristic differences exist between samples taken from either periodic or quasiperiodic structures.

R_L is usually calculated using transfer matrices: Let A_{in} , B_{refl} , and A_{trans} be the amplitudes of the incident, the reflected, and the transmitted electronic waves [cf. (20)] and let $\begin{pmatrix} R & S^* \\ S & R^* \end{pmatrix}$ be the transfer matrix mediating between the vectors $\begin{pmatrix} A_{\text{in}} \\ B_{\text{refl}} \end{pmatrix}$ and $\begin{pmatrix} A_{\text{trans}} \\ 0 \end{pmatrix}$. Then we have

$$R_L \propto \frac{|B_{\text{refl}}|^2}{|A_{\text{trans}}|^2} = |S|^2. \quad (24)$$

Many groups have investigated the dependence of $|S|^2$ on the energy and on the sample length. For approximants of growing length the $R_L(E)$ curves show increasingly rapid oscillation by many orders of magnitude.^{18,22} For nearly all energies R_L grows *exponentially* with sample length,¹⁸ whereas for the very few energies belonging to the spectrum (of the infinite quasilattice) the R_L growth is bounded by a power of the length.^{20,23,28} Goda

and Kubo²⁶ analyzed the generally exponential growth in more detail by numerically approximating the energy-dependent Lyapunov exponents

$$\gamma := \lim_{\text{length} \rightarrow \infty} \left[\frac{1}{\text{length}} \ln (|S|^2) \right].$$

Their $\gamma(E)$ curve consists of elliptic bumps of widely varying heights and widths. This plot strongly resembles the curve given by Würtz *et al.*²³ for the inverse localization lengths $\kappa(E)$ of the gap states.

Our main goal in the remaining discussion is to elucidate the relation between κ and γ and to give a simple estimate of the $R_L(E)$ dependence for growing samples. To bring out the characteristic effects of quasiperiodicity on the “resistances,” let us once again consider the successive approximants. We define the samples as one period of length P of each approximant. Note that a cyclic permutation of the sample geometry (e.g., from $LSLLS$ to $SLLSL$) generally distorts the $R_L(E)$ curve. To avoid misleading conclusions we shall always *average* over all the permutations, i.e., over different beginnings of the sampling period, instead of selecting one specific section by some arbitrary rule. This approach is in accord with Goda and Kubo’s calculations, whose Lyapunov exponents were also calculated as mean values from many different quasicrystal sections.

Since the TM’s $\begin{pmatrix} R & S^* \\ S & R^* \end{pmatrix}$ are complicated products of increasingly many single-interval matrices, their energy dependence can hardly be discussed analytically. Therefore we again switch to perturbation theory using the following two observations. First, the transfer matrix

describes at the same time the *finite* sample and its periodic extension, i.e., the whole approximant. Only the imposed boundary conditions distinguish between the scattering scenario considered here and the situation of Sec. III. Second, every TM—and consequently $|S|^2$ —can be reconstructed from its eigenvectors $\begin{pmatrix} A_{\pm} \\ B_{\pm} \end{pmatrix}$ and eigenvalues λ_{\pm} by means of its spectral decomposition. For the periodic approximants the vectors $\begin{pmatrix} A_{\pm} \\ B_{\pm} \end{pmatrix}$ and the values $\lambda_{\pm} = \exp(\pm i k_0 P)$ (for band energies) or $\lambda_{\pm} = \exp[i(k_0 \pm \kappa)P]$ (for gap energies) simply characterize the Bloch functions or the exponentially growing or decreasing states for the energy under consideration. Since we can deduce $A(x)$ and $B(x)$ from the wave functions [cf. (21)], it is possible to derive a perturbation series for the sought-after transfer matrices.

As we intend to explore the exponential R_L growth, and since the spectral energies tend to a set of zero measure, we restrict ourselves to the *gap energies*. Using the spectral decomposition of $\begin{pmatrix} R & S^* \\ S & R^* \end{pmatrix}$ we get

$$|S|^2 = \left| \frac{2B_+B_-}{A_+B_- - A_-B_+} \right|^2 \sinh^2(P\kappa). \quad (25)$$

Since the argument of the hyperbolic sine can become $\gg 1$ as we go to higher and higher approximants, it would not be wise to write down a perturbation series for the whole product given in (25). To take account of the exponential character of the hyperbolic sine we shall rather treat its argument and the squared fraction separately.

Let us recall the results of Sec. II B. The different states within the ℓ th gap were parametrized by $\phi \in (-\pi, \pi]$. Isoenergetic states are described by $\{\phi, -\phi\}$ and correspond to a pair $\{\kappa, -\kappa\}$. After some lengthy calculations based on (13) and (21) we get a very simple estimate for the prefactor of the hyperbolic sine:

$$\left| \frac{2B_+B_-}{A_+B_- - A_-B_+} \right|^2 = \frac{1}{\sin^2 \phi} + O(V). \quad (26)$$

Note that this expression is independent of the sample length and merely depends on the relative position of the energy within the gap. (This observation essentially remains valid in higher orders, but we shall not confuse the reader with the detailed formulas.) Consequently, the growth of R_L is determined by the hyperbolic sine, whence we conclude that the Lyapunov exponent γ should be identified with $2|\kappa|$ (the factor 2 arises from the *squared* sinh).

However, this conclusion presupposes that, for a given energy, κ is independent of the sample length P . This point needs further discussion. Since the electronic spectra of successive approximants differ, the gap regions where $\kappa \neq 0$ actually depend on the periods P . On the other hand, gaps which are open in some approximant, remain open in all following approximants with almost unchanged positions and widths. Furthermore, the κ values inside these “common” gaps also hardly change. To explain this fact let us recall the elliptic relation (15) and (16) of κ and E (which remains almost unchanged in higher orders and is confirmed by TM calculations):

$$\begin{pmatrix} \kappa \\ E \end{pmatrix} = \begin{pmatrix} \frac{|\hat{V}_{\ell}|}{2k_0} \sin \phi \\ k_0^2 + \hat{V}_0 + |\hat{V}_{\ell}| \cos \phi \end{pmatrix} + O(V^2). \quad (27)$$

Now the above observations are reduced to the known fact that for any \hat{V}_{ℓ} peak of some given approximant there is always a Fourier peak of nearly identical magnitude and wave vector for any higher approximant, whence (27) predicts a practically stationary $\kappa(E)$ ellipse. As we go to higher approximants, smaller and smaller new gaps open up between the “old” ones, adding tiny new ellipses, but hardly affecting the preexisting ones. This scenario is illustrated in Fig. 5. In the limit of an infinite quasilattice we would arrive at a dense succession of elliptic κ bumps of widely varying sizes. But this is just what was suggested by the plots of Würtz *et al.*²³ and of Goda

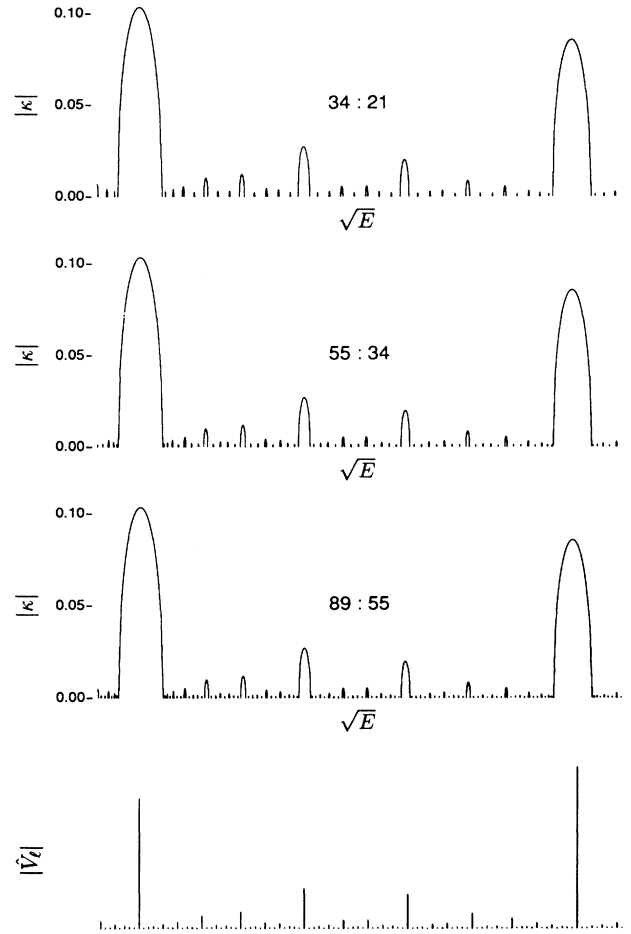


FIG. 5. Evolution of the increasingly dense succession of κ ellipses within the gaps for a sequence of Fibonacci approximants. (The curves were calculated using TM's for $V = 1$ and $3.1 \leq \sqrt{E} \leq 5.4$.) The important point to be observed is that once a κ ellipse has come into existence it remains almost unchanged in the $\kappa(E)$ curves of the following approximants. The bottom plot presents the corresponding section of the Fourier spectrum of the 89:55 approximant. The correspondence between the sizes of the ellipses and the Fourier coefficients $|\hat{V}_{\ell}|$, as expressed in (27), is evident.

and Kubo.²⁶ Here, apart from explaining the origin of this type of $\kappa(E)$ or $\gamma(E)$ dependence, we have come to the handy interpretation of the heights and widths of the ellipses as a “fingerprint” of the samples’ Fourier spectra.

Since the Lyapunov exponents only partially describe the resistances, let us conclude with a brief discussion of their absolute values; see Fig. 6. Combining (25)–(27) we get the following lowest-order estimate for the ℓ th gap:

$$|S|^2 \simeq \frac{\sinh^2\left(\frac{P|\hat{V}_\ell|}{2k_0} \sin\phi\right)}{\sin^2\phi}. \quad (28)$$

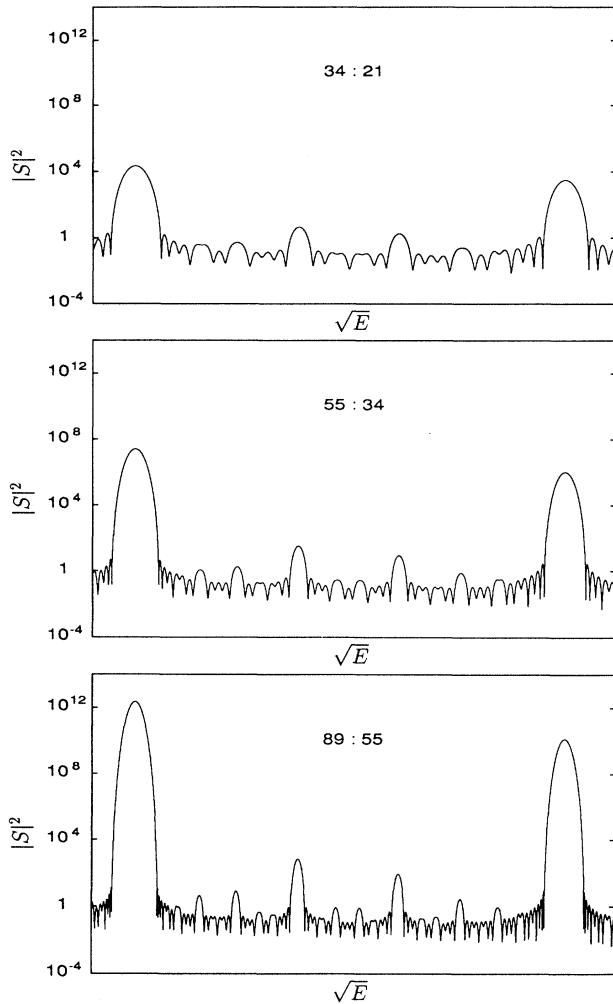


FIG. 6. Evolution of the resistances for the same approximants as in Fig. 5. $|S|^2$ was averaged over all possible samples of length 55, 89, or 144, respectively; see the text. Note the logarithmic ordinate scale. Two things should be observed. First, inside the larger gaps $|S|^2$ grows exponentially with increasing sample length in full accord with the κ plots of Fig. 5. Second, we always find energies with “almost resonant transmission,” i.e., $|S|^2 \ll 1$. These R_L minima correspond to the “youngest” gaps with smallest $|\hat{V}_\ell|$; compare also the caption of Fig. 7.

Traversing the gap, $|S|^2$ approximately takes on values between $P^2 \frac{|\hat{V}_\ell|^2}{4k_0^2}$ (at the band edges) and $\sinh^2\left(\frac{P|\hat{V}_\ell|}{2k_0}\right)$ (at the gap’s center). Note that this estimate does *not* allow any arbitrary scaling, i.e., the values given by (28) directly yield the correct orders of magnitude of the resistances. (This is contrary to the wave functions, which are suitably normalized after the approximation.) The success of our estimates is demonstrated in Fig. 7.

It might be noteworthy that many dips of the R_L curves are due to tiny gaps, for which $(P\kappa)$ is not yet big enough to expose the exponential character of the hyperbolic sine. That this will always happen for the smallest gaps without restrictions to the sample length is suggested by the explicit formula for the Fourier transform of an approximant, which we state without proof:³⁴

$$|\hat{V}_\ell| = V \left| \frac{\sin(P\ell\Phi)}{P \sin(\ell\Phi)} \right|, \quad (29)$$

where Φ can be calculated from the continued fractions expansion of $p:q$. The smallest gaps correspond to those indices ℓ for which $\sin(\ell\Phi)$ is of the order of ± 1 , whence

$$\left| \frac{P\hat{V}_\ell}{2k_0} \right| \lesssim \left| \frac{V}{2k_0} \right| \implies |S|^2 \lesssim \sinh^2\left(\frac{V}{2k_0}\right).$$

This behavior has a counterpart in “periodic” samples. Considering a succession of P identical elementary cells of unit length, Vezzetti and Cahay³⁷ showed that perfect “resonant” transmission occurs for all energies corresponding to Bloch wave vectors $k_0 = \frac{\ell\pi}{P}$, $\frac{\ell}{P} \notin \mathbb{Z}$. This

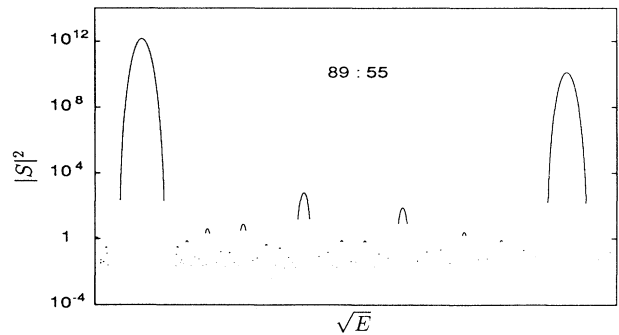


FIG. 7. The results of perturbation theory for $|S|^2$ within the gaps. In order to correctly shift the energetic gap positions in the vicinity of large gaps, the depicted curve was calculated to second order. A thorough comparison with Fig. 6 reveals convincing agreement. Omitting the interpolating curve segments for the band energies brings out the large resistance fluctuations as we run through the successive gaps. Note the coexistence of large gaps with the typical $|S|^2$ maxima and tiny gaps where the full $|S|^2$ curve has dips; see the text. (The omitted $|S|^2$ maxima from the band regions between the smallest gaps can also be accounted for by perturbation theory. For details see Ref. 34.)

result nicely confirms (28) since for a sample consisting of P identical unit cells we have $\hat{V}_\ell = 0$ for $\frac{\ell}{P} \notin \mathbb{Z}$.³⁸ We can thus interpret the smallest Fourier coefficients in (29) as remnants of the vanishing \hat{V}_ℓ 's as we gradually shift the equidistant potential peaks towards the vertices of our approximants.

Summarizing, we always find gaps (which have opened up some generations ago) where the resistances grow exponentially with Lyapunov exponents as discussed at the beginning, and other "young" gaps where the R_L curves show local minima. These, however, yield to an exponential R_L growth as we grow larger samples, while at the same time even smaller new gaps open up, where the transmission is again quite good.

V. SUMMARY

The first part of our work complements the known, rigorously proven facts about quasiperiodic Hamiltonians by an analysis of the typically non-self-similar wave functions. A comparison for successive rational approximants showed that local shapes of the Bloch functions of lower approximants reappear as constituents of the more complicated states of higher approximants. Using perturbation theory we were able to derive an approximate description for the envelopes of the wave functions which allowed a simplified discussion of the observed structural hierarchy. Moreover, our model accounts for the fact that the corresponding states are always most similar around the common symmetry centers of the compared approximants. These findings may help to think about the seemingly chaotic states of huge approximants (or even quasicrystals) as a result of an iterative building process, in which the assembly of increasingly complex states of the growing approximants reflects the geometric concatenation rule (19).

In the second part we discussed the complicated dependence of the Landauer resistance on energy and sample length. First, we presented an argument that intimately links the inverse localization lengths κ of the gap states and the Lyapunov exponents γ of the R_L growth with sample length. Using our perturbation theory for the gap states we then interpreted the distribution of the $\kappa(E)$ values as a fingerprint of the samples' Fourier spectra. Guided by the simple formula (28) for R_L we were able to extract the distinct contributions from the successive gaps within the complicated $R_L(E)$ curves. These reflect in a very elementary way the broad distribution of the approximants' Fourier coefficients. Thus we got some fundamental insights into the evolution of the increasingly complex R_L curves as we go to larger samples.

It is not yet clear to what extent the now known properties of linear quasiperiodic Hamiltonians remain valid for higher dimensional systems. Besides lacking simple analytic tools such as the TM method or the concept of the Landauer resistance as expressed in (24), some studies of tight-binding models indicate possible qualitative differences, e.g., for the localization of the wave functions.^{5,39} We are still far from a realistic understanding of the physical consequences of quasiperiodicity.

APPENDIX: REFORMULATION OF PERTURBATION THEORY

Let us discuss the nondegenerate case first. In order to calculate the successive orders of ψ and E we substitute (3) into (1) and collect all terms of order $O(V^n)$:

$$-\frac{d^2}{dx^2} \psi^{(0)}(x) = E^{(0)} \psi^{(0)}(x), \quad (\text{A1})$$

$$-\frac{d^2}{dx^2} \psi^{(n)}(x) + V(x) \psi^{(n-1)}(x) = \sum_{k=0}^n E^{(k)} \psi^{(n-k)}(x) \quad (n > 0). \quad (\text{A2})$$

(A1) is solved by

$$\psi^{(0)}(x) = \exp(i k_0 x), \quad E^{(0)} = k_0^2. \quad (\text{A3})$$

Since Bloch functions are exclusively composed of plain waves with wave vectors $k_m := k_0 + \frac{2\pi m}{P}$, it is common to treat the problem in Fourier space by writing

$$\psi(x) = \sum_{m \in \mathbb{Z}} \hat{\psi}_m \exp(i k_m x).$$

The successive corrections of ψ are calculated from the Fourier transform of (A2). Keeping the Fourier coefficient $\hat{\psi}_0$ fixed and using (A3) we arrive at

$$\hat{\psi}_m^{(n)} = \hat{f}_m \cdot \hat{h}_m^{(n)} \quad (\text{A4})$$

with

$$\hat{f}_0 := 0, \quad \hat{f}_m := \frac{1}{k_0^2 - k_m^2} \quad (m \neq 0), \quad (\text{A5})$$

$$\begin{aligned} h^{(n)}(x) &= \sum_{m \in \mathbb{Z}} \hat{h}_m^{(n)} \exp(i k_m x) \quad (\text{A6}) \\ &= V(x) \psi^{(n-1)}(x) - \underbrace{\sum_{k=1}^{n-1} E^{(k)} \psi^{(n-k)}(x)}_{:=0 \text{ for } n=1}. \end{aligned}$$

Note that the \hat{f}_m are *independent* of the order n .

The essential point is that we can backtransform the *whole infinite set* (A4) into real space using the convolution theorem as soon as the Fourier transform of $\{\hat{f}_m\}$ is calculated:

$$\begin{aligned} f(x) &= \exp(i k_0 x) \left\{ \frac{-1}{4k_0^2} + i \frac{2x - P}{4k_0} \right. \\ &\quad \left. + \frac{P \exp[ik_0(P - 2x)]}{4k_0 \sin(Pk_0)} \right\} \quad (0 \leq x \leq P) \\ \implies \psi^{(n)}(x) &= \frac{1}{P} \int_0^P f(x') h^{(n)}(x - x') dx'. \end{aligned}$$

To calculate the energy corrections we make use of the fact that $\psi^{(0)}$ and $\psi^{(n)}$ ($n > 0$) have disjoint Fourier support and are thus orthogonal over the interval $[0, P]$.

Multiplying (A2) by $\psi^{(0)*}$ and integrating yields

$$E^{(n)} = \frac{1}{P} \int_0^P V(x) \psi^{(n-1)}(x) \exp(-i k_0 x) dx. \quad (\text{A7})$$

Note that no infinite sums are to be evaluated here. The results (5)–(9) follow from (A6)–(A7).

Now we turn to the gap states. First, substituting the ansatz (10) into (1), we get

$$\left[-\kappa^2 - 2\kappa \frac{d}{dx} - \frac{d^2}{dx^2} + V(x) \right] w(x) = E w(x). \quad (\text{A8})$$

Since $w(x)$ is of the Bloch type (11) we can write

$$w(x) = \sum_{m \in \mathbb{Z}} \hat{w}_m \exp(i k_m x).$$

Now, since $k_0 = -k_{-\ell} = \frac{\ell\pi}{P}$, the unperturbed problem

$$(k_m^2 - E^{(0)}) \hat{w}_m^{(0)} = 0, \quad E^{(0)} = k_0^2$$

is solved by

$$\hat{w}_0^{(0)}, \hat{w}_{-\ell}^{(0)} = (\text{undetermined}), \quad \hat{w}_m^{(0)} = 0 \quad (m \neq 0, -\ell).$$

To determine the ratio $\hat{w}_0^{(0)} : \hat{w}_{-\ell}^{(0)}$ we have to look at the first-order terms of (A8). The Fourier coefficients for $\exp(\pm i k_0 x)$ yield

$$\begin{pmatrix} [\hat{V}_0 - \Theta] & \hat{V}_\ell \\ \hat{V}_\ell^* & [\hat{V}_0 - \Theta^*] \end{pmatrix} \begin{pmatrix} \hat{w}_0 \\ \hat{w}_{-\ell} \end{pmatrix} \stackrel{!}{=} \begin{pmatrix} 0 \\ 0 \end{pmatrix}, \quad (\text{A9})$$

where we have defined $\Theta := E^{(1)} + 2i k_0 \kappa^{(1)}$. Assuming a *symmetric* potential as in (12), the solutions of (A9) can be parametrized as follows:

$$E^{(1)} + 2i k_0 \kappa^{(1)} = \hat{V}_0 + \exp(i\phi) |\hat{V}_\ell|, \quad (\text{A10})$$

$$\hat{w}_0^{(0)} = \hat{w}_{-\ell}^{(0)*} = \alpha \exp\left(-i \left[k_0 x_s + \frac{\phi}{2} \right]\right), \quad (\text{A11})$$

with $\alpha = \frac{1}{2}$ for $\hat{V}_\ell^s > 0$ and $\alpha = \frac{-i}{2}$ for $\hat{V}_\ell^s < 0$. For $\phi = 0, \pi$ we retrieve the well-known expressions for the band edges, i.e., $E^{(1)} = \hat{V}_0 \pm |\hat{V}_\ell|$. Splitting (A10) into its real and imaginary parts we get (15) and (16).

To derive the higher-order corrections we proceed as before. The general result for w is

$$w^{(n)}(x) = \frac{1}{P} \int_0^P f(x') h^{(n)}(x - x') dx', \quad (\text{A12})$$

with new functions f and $h^{(n)}$:

$$f(x) = \frac{-\cos(k_0 x)}{2k_0^2} + \sin(k_0 x) \frac{P - 2x}{2k_0} \quad (0 \leq x \leq P),$$

$$h^{(n)} = V w^{(n-1)} - \underbrace{\sum_{k=1}^{n-1} \sum_{j=1}^{k-1} \kappa^{(j)} \kappa^{(k-j)} w^{(n-k)}}_{:=0 \text{ for } n \leq 2} - \underbrace{\sum_{k=1}^{n-1} E^{(k)} w^{(n-k)} - 2 \sum_{k=1}^{n-1} \kappa^{(k)} \frac{dw^{(n-k)}}{dx}}_{:=0 \text{ for } n=1}.$$

The new form of f arises from fixing not only \hat{w}_0 , but also $\hat{w}_{-\ell}$, i.e., from redefining $\hat{f}_{-\ell} := 0$ in (A5). Note, however, that for *nonsymmetric* potentials the ratio $\hat{w}_0 : \hat{w}_{-\ell}$ may change as we go to higher orders so that we have to modify (A12); cf. Ref. 34. For completeness we give the κ and E corrections for $n \geq 2$:

$$E^{(n)} = \frac{2}{P} \int_0^P \left[w^{(0)} V w^{(n-1)} \right] (x) dx - \sum_{k=1}^{n-1} \kappa^{(k)} \kappa^{(n-k)},$$

$$\kappa^{(n)} = \frac{1}{P k_0^2} \int_0^P \left[\frac{dw^{(0)}}{dx} V w^{(n-1)} \right] (x) dx,$$

where $w^{(0)}(x) = \text{trig} \left[k_0 (x - x_s) - \frac{\phi}{2} \right]$ with $\text{trig} := \cos$ (sin) for $\hat{V}_\ell^s > 0$ (< 0) due to (A11).

- ¹ D. Shechtman, I. Blech, D. Gratias, and J. W. Cahn, Phys. Rev. Lett. **53**, 1951 (1984).
- ² T. Ishimasa, H.-U. Nissen, and Y. Fukano, Phys. Rev. Lett. **55**, 511 (1985).
- ³ L. Bendersky, Phys. Rev. Lett. **55**, 1461 (1985).
- ⁴ B. D. Biggs, S. J. Poon, and N. R. Munirathnam, Phys. Rev. Lett. **65**, 2700 (1990).
- ⁵ H. Böttger and G. Kasner, Phys. Status Solidi B **164**, 11 (1991).
- ⁶ A. E. Carlsson, Nature **353**, 15 (1991).
- ⁷ S. J. Poon, Adv. Phys. **41**, 303 (1992).
- ⁸ C. Janot, *Quasicrystals: A Primer* (Clarendon Press, Oxford, 1992), Chap. 6.4.
- ⁹ H. Akiyama *et al.*, J. Phys. Soc. Jpn. **62**, 639 (1993).
- ¹⁰ F. S. Pierce, S. J. Poon, and Q. Guo, Science **261**, 737 (1993).
- ¹¹ F. S. Pierce, S. J. Poon, and B. D. Biggs, Phys. Rev. Lett. **70**, 3919 (1993).

- ¹² M. A. Chernikov, A. Bernasconi, C. Beeli, and H. R. Ott, Europhys. Lett. **21**, 767 (1993).
- ¹³ B. Simon, Adv. Appl. Math. **3**, 463 (1982).
- ¹⁴ J. Bellissard and E. Scoppola, Commun. Math. Phys. **85**, 301 (1982).
- ¹⁵ S. Ostlund *et al.*, Phys. Rev. Lett. **50**, 1873 (1983).
- ¹⁶ M. Kohmoto, L. P. Kadanoff, and C. Tang, Phys. Rev. Lett. **50**, 1870 (1983).
- ¹⁷ M. Kohmoto and Y. Oono, Phys. Lett. **102A**, 145 (1984).
- ¹⁸ J. Kollár and A. Sütó, Phys. Lett. A **117**, 203 (1986).
- ¹⁹ M. Kohmoto, B. Sutherland, and C. Tang, Phys. Rev. B **35**, 1020 (1987).
- ²⁰ B. Sutherland and M. Kohmoto, Phys. Rev. B **36**, 5877 (1987).
- ²¹ M. Holzer, Phys. Rev. B **38**, 1709 (1988).
- ²² S. D. Sarma and X. C. Xie, Phys. Rev. B **37**, 1097 (1988).
- ²³ D. Würtz, M. P. Soerensen, and T. Schneider, Helv. Phys. Acta **61**, 345 (1988).

- ²⁴ J. Bellissard, B. Iochum, E. Scoppola, and D. Testard, *Commun. Math. Phys.* **125**, 527 (1989).
- ²⁵ T. Fujiwara, M. Kohmoto, and T. Tokihiro, *Phys. Rev. B* **40**, 7413 (1989).
- ²⁶ M. Goda and H. Kubo, *J. Phys. Soc. Jpn.* **58**, 2109 (1989).
- ²⁷ A. Sütő, in *Number Theory and Physics*, edited by J. M. Luck, P. Moussa, and M. Waldschmidt, Springer Proceedings in Physics Vol. 47 (Springer-Verlag, Berlin, 1990), pp. 162–169.
- ²⁸ B. Iochum and D. Testard, *J. Stat. Phys.* **65**, 715 (1991).
- ²⁹ M. Baake, D. Joseph, and P. Kramer, *Phys. Lett. A* **168**, 199 (1992).
- ³⁰ M. Baake, U. Grimm, and D. Joseph, *Int. J. Mod. Phys. B* **7**, 1527 (1993).
- ³¹ J. M. Luck, *Phys. Rev. B* **39**, 5834 (1989).
- ³² D. Barache and J. M. Luck, *Phys. Rev. B* **49**, 15 004 (1994).
- ³³ J. M. Luck and D. Petritis, *J. Stat. Phys.* **42**, 289 (1986). Keeping in view the coordinate origin in the two- to one-dimensional projection formalism, a modified concatenation rule is given by the authors, but the simpler formula (19) yields merely permuted elementary cells.
- ³⁴ J. Peters, Ph.D. thesis, Universität Stuttgart, 1994.
- ³⁵ For $p:q$ approximants with $p \geq q$ one never finds two adjoining S intervals. Therefore, no type D centers between two S intervals exist.
- ³⁶ For the exact wave functions the difference $|A|^2 - |B|^2$ is a *constant* independent of x . This is a consequence of current conservation and follows immediately from TM calculations. Starting with a right-traveling wave as in (4) for the unperturbed problem, $|A|$ will always exceed $|B|$, whence $|\Delta|A|| < |\Delta|B||$.
- ³⁷ D. J. Vezzetti and M. M. Cahay, *J. Phys. D* **19**, L53 (1986).
- ³⁸ Here the whole sample is regarded as an elementary cell of a superstructure with period P and the Fourier coefficients are defined as $\hat{V}_\ell = \frac{1}{P} \int_0^P \exp(-i\frac{2\pi\ell}{P}x) V(x) dx$.
- ³⁹ P. Ma and Y. Liu, *Phys. Rev. B* **39**, 9904 (1989).